AIAA JOURNAL
Vol. 36, No. 3, March 1998

Force Measurements in Hypersonic Impulse Facilities

V. Störkmann,* H. Olivier,† and H. Grönig‡
Rheinisch–Westfälische Technische Hochschule, 52056 Aachen, Germany

A six-component strain gauge balance is used to measure aerodynamic loads of different models in hypersonic wind tunnels with running times down to 1 ms. Three models are employed, a pointed cone, an Apollo CM capsule, and a delta wing configuration, ELAC I. All models are tested in the Aachen shock tunnel TH2; the capsule model was additionally tested in the von Kármán Institute Longshot facility. Two different methods are applied to compensate for low-frequency inertia forces caused by the model support system for the capsule tests. The measured aerodynamic coefficients are compared with experimental and numerical values of other authors.

Nomenclature

a = acceleration
C^* = Chapman Rubesin factor
c = aerodynamic coefficient, $[F(M)/(\rho_\infty/2)u_\infty^2 S_{\text{ref}}(l_{\text{ref}})]$
D = maximum diameter of command module
F = aerodynamic force
k = dynamic pressure factor, $[(\rho_\infty/2)u_\infty^2/p_{t2}]$
L = length of center chord
l_{ref} = reference length of moment coefficients
M = aerodynamic moment
M_∞ = freestream Mach number
Re = Reynolds number
S_{ref} = reference area
$\bar{V}^*$ = viscous interaction parameter, $M_\infty(\sqrt{C^*}/\sqrt{Re})$
Z = total balance loads
α = angle of attack
ϵ = 90 deg $-$ Λ
Λ = leading-edge sweep angle, 75 deg

Subscripts

a = axial
D = drag
g = center of gravity
L = lift
M_y = pitching moment
m = model
n = normal
t = stagnation conditions
0 = nozzle reservoir state
1 = driven tube initial state
4 = driver tube initial state
∞ = freestream condition

I. Introduction

FORCE measurements in high-enthalpy wind tunnels are restricted by the short duration the steady flowfield can be sustained. Typical values for the flow duration achieved range from 0.5 to 10 ms. Because of the sudden impact of the aerodynamic forces on the model and its support, the complete system starts oscillating with its natural frequencies. The resulting inertia forces of both the model and the balance add to the aerodynamic forces and moments. Measuring forces in conventional wind tunnels, the useful test time starts when these oscillations are damped down and the system remains in a steady state. This is not possible in short-duration facilities because there is almost no damping in the few milliseconds of flow duration.

In the past, several methods have been developed to overcome these problems. Naumann et al.[1] developed a method to measure the accelerations of a free flying model in a shock tunnel. The model is controlled by a mounting support that releases the model for some milliseconds just before the onset of the flow. As there are no connecting parts between the model and the support system, there are no accelerations caused by this system. The forces are derived from the accelerations and the inertia matrix of the model by applying Newton's law. It is necessary to have the model equipped with six or more accelerometers, and the inertia matrix of the model has to be determined in each individual case.

Mee et al.[2] are working with a model that is connected to a long hollow sting. This setup hangs in the wind tunnel on two shielded wires and may freely move in the flow direction as well as pitch and positively lift. Instead of the accelerations the stress waves are measured introduced into the system. The aerodynamic forces are derived from the measured stress waves via nine impulse response functions that have to be determined by a series of step loads applied to the model. The accurate determination of these response functions is very important because they have to replace the static calibration and the compensation of possible oscillations.

Jessen and Grönig[3] presented a strain gauge balance that was designed to work without an acceleration compensation at all. In combination with a model of sufficiently high stiffness and low moment of inertia, this six component balance achieves natural frequencies of about 1 kHz. Because the balance is part of the sting it is virtually independent of the model and may be calibrated statically with high accuracy. The models for this balance do not need any acceleration gauges installed inside, and no inertia matrix has to be determined. Although the response time of this balance in combination with a model is short enough to measure the aerodynamic coefficients within the test time, the model support contributes low-frequency oscillations ($\leq$200 Hz) to the system. The resulting inertia forces add to the aerodynamic forces.

In the present paper different methods for compensating for these inertia forces are compared and results for different models (pointed cone, Apollo command module capsule, and ELAC I) are presented.

II. Short Description of the Experimental Facilities

A. Aachen Shock Tunnel TH2

The shock tunnel TH2 operates in the reflected mode. The shock tube has an inner diameter of 140 mm; the length of driver and driven section are 6 and 15.4 m, respectively. The maximum driver pressure reaches 150 MPa and a maximum temperature of 600 K. With helium as driver and artificial air as test gas, nozzle reservoir conditions are achieved from 1.5 to 63 MPa at temperatures between 1500 and 4700 K (Ref. 4). For the experiments presented, a conical nozzle has been used with 586-mm exit diameter and 5.8-deg half-angle. Depending on the nozzle area ratio, which can be changed by different throat inserts, the reservoir gas is expanded to freestream Mach numbers between 6.5 and 12. For the force measurements presented, Table 1 gives the conditions I, IV, and VII used.

Received May 21, 1997; revision received Nov. 11, 1997; accepted for publication Nov. 11, 1997.

*Research Scientist, Shock Wave Laboratory, Templergraben 55.
†Professor, Shock Wave Laboratory, Templergraben 55. Member AIAA.
‡Professor Emeritus, Shock Wave Laboratory, Templergraben 55. Senior Member AIAA.

Table 1 Operating conditions of TH2

Condition	p_4, MPa	T_4, K	p_1, MPa	p_0, MPa	T_0, K	h_0, MJ/kg	M_∞	Re_∞, 10^6/m	Test gas	$\bar{V}^*$[a]
I	10	293	0.1	6.5	1500	1.7	7.9	4.3	Air	0.0108
IV	120	573	0.06	51	4700	6.8	6.3	3.8	Air	0.0093
VII	130	573	0.07	63	4600	6.6	12.1	0.5	Air	0.036

[a]Note $l = 0.12$ m.

Table 2 Operating conditions of VKI Longshot

Condition	p_4, MPa	T_4, K	p_1, MPa	p_0, MPa	T_0, K	M_∞	Re_∞, 10^6/m	Test gas	$\bar{V}^*$[a]
LSCN 1	34.4	293	0.235	95	2000	15	7.5	N_2	0.0130
LSCN 2	34.4	293	0.227	130	2000	11.2	6.7	CO_2	0.0130
LSCN 3	34.4	293	0.144	50	1900	14.8	4.2	N_2	0.0200
LSCN 4	34.4	293	0.227	225	2250	13.3	4.6	CO_2	0.0200

[a]Note $l = 0.12$ m.

B. von Kármán Institute Longshot Wind Tunnel

The Longshot facility at the von Kármán Institute (VKI) in Brussels operates as a piston gun tunnel. It consists of a driver tube with 125-mm inner diameter, 6 m long, and a 75-mm-inner-diameter driven tube, 27 m long, separated from the high-pressure reservoir/hypersonic nozzle system by a set of 48 check valves. Nylon pistons are used with a steel or titanium core of 1.5–9 kg weight. They are accelerated by the driver gas (nitrogen, 30–100 MPa) to a speed of the order of 600 m/s. The driven tube is initially filled with 0.1–1.5 MPa of nitrogen or carbon dioxide. This gas is compressed by the piston to nozzle reservoir conditions up to 400 MPa at 2500 K (Ref. 5). Table 2 gives the detailed operating variables of the four conditions used for the 120-mm capsule model.[6] These four conditions were chosen to investigate the effects of variations in γ for constant values of the rarefaction parameter $\bar{V}^*$. The value of γ is changed by the use of nitrogen or carbon dioxide as test gas.

III. Six-Component Strain Gauge Balance

For the current study a sting mounted strain gauge balance is used that was developed by Jessen and Grönig.[3] It measures all six components of the aerodynamic load in a configuration that is shaped like a cross (Fig. 1). The center of this cross is rigidly connected to the balance sting (not shown in the figure) by means of thermal shrinking. The outer ends of the arms carry a cylindrical shell, which connects to the cone of the model mount. The balance is manufactured from one piece of stainless steel (17-4-PH, yield strength $>1200\,\mathrm{N/mm^2}$) to minimize all hysteresis effects. A total of 32 semiconductor strain gauges is installed to measure the deformations of the four cross arms, which can be assigned to the six load components. The balance is not designed for a minimum crosstalk between the six components but for a maximum stiffness for measuring without a model-based acceleration compensation. The lowest natural frequency of this balance is that of the pitching moment of about 2.3 kHz. This resonance frequency is considerably lowered by the inertia of the model. The comparatively large interferences ($\leq 5\%$) require a calibration matrix that also takes into account third-order terms.[7] The relation between signal and load is given by

$$S_i = R_{0i} + \sum_{j=1}^{6} a_{ij} Z_j + \sum_{j=1}^{6} \sum_{k=j}^{6} b_{ijk} Z_j Z_k + \sum_{j=1}^{6} c_{ij} Z_j^3 \qquad i = 1, 2, \ldots, 6 \quad (1)$$

where S_i is the output of the strain gauge bridge of component i, R_{0i} the output of bridge i without load, Z_j the total load acting on component j, a_{ij} the calibration factors for linear terms, b_{ijk} the calibration factors for square terms, and c_{ij} the calibration factors for cubic terms. The calibration coefficients are calculated from the data of a static calibration by means of a least squares fit. The S_i are the measured and digitized quantities during an experiment. As the Z_j are the unknowns, the preceding nonlinear set of equations has to be solved for each set of six values S_i recorded at a certain instant. This is achieved using Newton's method for a set of nonlinear equations. The balance is calibrated in a range of ± 500 N for all forces and ± 25 Nm for the moments. The axial force that is needed for a plastic deformation of 0.2% is approximately 16.5 kN. The measuring range of the balance may be optimized for a specific model by adjusting the exitation voltage (5−15 V) and the signal amplification (up to 10,000 times) of each component.

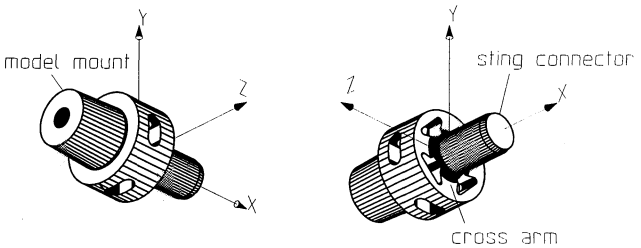

Fig. 1 Strain gauge balance.

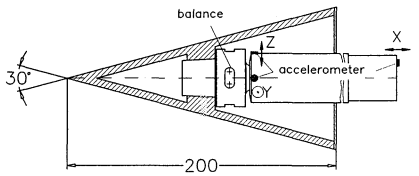

Fig. 2 Cone model with installed balance.

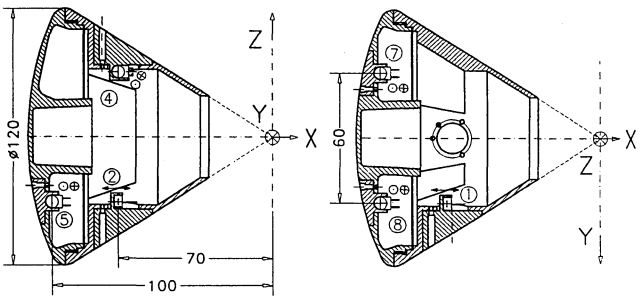

Fig. 3 Geometry of the capsule model with accelerometer positions (dimensions in millimeters).

IV. Models Used for Force Measurements

A. Pointed Cone

The pointed cone model has an apex angle of 30 deg and a length of 200 mm (Fig. 2). It is machined from FORTAL aluminum (AlZnMgCu 0.5). The model mass is 328 g, and the main moment of inertia is $995\,\mathrm{kgmm^2}$ with respect to the balance fixed coordinate system. This configuration was chosen for its easy design and for the possibility to compare the results with theoretical and experimental literature values.[8–10] The coefficients are related to the cone base area S_{ref}, and the pitching moment refers to the cone tip, where l_{ref} is the cone length.

B. Apollo Command Module Capsule

The geometry of the capsule model used for testing is based on the basic configuration of the Apollo command module.[11] It has a maximum diameter of $D = 120$ mm and is equipped with six accelerometers to perform a model-based acceleration compensation in addition to the sting-based compensation. The model is built from FORTAL aluminum. The positions of the accelerometers, including their sensing direction and the model geometry, are given in Fig. 3. To fit the balance into the model, the conical rear part of the capsule was shortened by 12 mm, which leads to a diameter of the frustum of 37 mm. The diameter of the balance sting is 36 mm, which results in a clearance of 0.5 mm between model and balance sting. This cutoff probably increases the determined drag coefficients. The model mass amounts to 455 g with a main moment of inertia of $830\,\mathrm{kgmm^2}$ with respect to the balance-fixed coordinate system. Mounted on the balance the lowest natural frequency of this system is about 720 Hz. As already mentioned, the signals measured with this model may be processed in two different ways, with or without a model-based

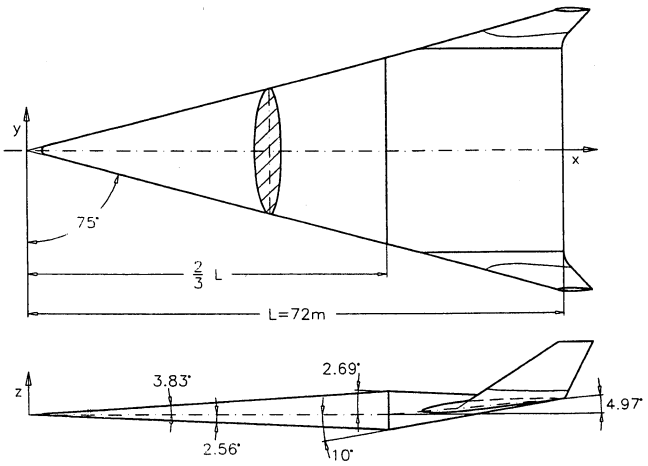

Fig. 4 Geometry of ELAC I.

acceleration compensation, and the two results may be compared. All aerodynamic coefficients are given in a body-fixed coordinate system with $S_{\text{ref}} = \pi D^2/4$, the moments are calculated for the chosen reference point with the coordinates $X_g = -0.6664D$, $Y_g = 0$, and $Z_g = -0.0353D$, which is close to the center of gravity of the Apollo capsule, with $l_{\text{ref}} = D$ (Fig. 3).

C. ELAC I

This model represents a simplified configuration of the lower stage of a two-stage space transportation system investigated by the Collaborative Research Center, Fundamentals of the Design of Aerospace Planes, at the Aachen University of Technology. It is shaped like a thick delta wing with two winglet type rudders (Fig. 4). For the shock-tunnel measurements a model is used at a scale of 1:240 ($L_m = 0.3$ m). The maximum height of this model is 22 mm which makes it impossible to install the balance inside of the model. It has to be installed as an external sting balance. Even with very light models this leads to high moments of inertia due to the relatively large distance between the center of gravity and the balance. For the force measurements, a model made of carbon fiber reinforced plastic has been built to make it as light as possible. It weighs 220 g, and the moment of inertia is approximately 5800 kgmm^2 with respect to the balance-fixed coordinate system. This high value results mainly from the external position of the balance. In this case the resonance frequency is 140 Hz, which is in the same range as the support system oscillations. Thus, it is not possible to perform force measurements without a model-based acceleration compensation for measuring times less than 8 ms. The coefficients given for this model refer to the planform area S_{ref} of the delta wing; the reference length of the pitching moment coefficient is $\frac{2}{3}L_m$. It is related to the moment reference point at $X = L_m/2$.

V. Compensation of Inertia Forces

The balance system was originally designed to work without any acceleration compensation. It is as stiff as possible but still with a sufficient sensitivity for all six components. With a model moment of inertia of less than 750 kgmm^2 with respect to the balance-fixed coordinate system, the resulting lowest natural frequencies are higher than 1 kHz. This is sufficient for test times down to 1 ms.

A. Balance Sting-Based Acceleration Compensation

In the real test environment, however, the reaction of the model support is not ideal, i.e., it is oscillating during the test time together with the model-balance system. In the regular case these oscillations show a lower frequency than those of the model-balance system. For the shock tunnel TH2 the model support system is oscillating with a main frequency of about 200 Hz. At the VKI Longshot the model support oscillations take place at about 80 Hz. These frequencies are too low for reading a steady value of the forces and moments during the measuring time. For this reason an acceleration compensation of the model support oscillations is necessary. It would be convenient to compensate for the forces induced by these oscillations by measuring the accelerations of the balance sting because this procedure would be independent from the model. Assuming a linear relation between acceleration and corresponding force without any interference, the relations are

$$F_i = Z_i - m_i \cdot a_i, \qquad i = x, y, z \tag{2}$$

$$M_i = Z_{Mi} - m_{Mi} \cdot a_j, \qquad i = y, z, \qquad j = z, y \tag{3}$$

where F_i and M_i are the aerodynamic loads, Z_i and Z_{Mi} the measured interference corrected balance signals, a_i and a_j the measured sting accelerations, and m_i and m_{Mi} the unknown factors, which represent a combination of the oscillating masses, i.e., of the model and a part of the balance. This holds for three accelerometers, one in each direction with the measuring axis aligned to the coordinate system. With this configuration it is not possible to measure an angular acceleration that is proportional to the rolling moment. Fortunately, low-frequency oscillations of the component M_x have not been observed, so that it is not necessary to compensate this component.

The unknown factors m_i and m_{Mi} depend on the model and on the frequency for which they are used. The frequency of the model support system depends on the model and the specific angle of attack that influences the geometry and therewith the dynamic behavior of the support system. This leads to the conclusion that these factors have to be determined for each single test with the model mounted in the test section. This makes it necessary to measure them in a convenient way. A possibility to obtain the measurements is to let the system oscillate without any aerodynamic forces. The excitation of the system with an impulse hammer leads to oscillations around the zero line without aerodynamic forces with a short leading force pulse that is measured by the hammer and the balance. In this case relations (2) and (3) become

$$Z/a = m \tag{4}$$

or, because the system is oscillating around the zero line, the calculation can be done with rms values. A time-dependent rms value is calculated for both signals according to

$$Z_{\text{rms}} = \sqrt{\sum_{k-n}^{k+n} Z^2 \Big/ (2n+1)}, \qquad a_{\text{rms}} = \sqrt{\sum_{k-n}^{k+n} a^2 \Big/ (2n+1)}$$

$$\text{with} \quad 1 + n \le k \le N - n \tag{5}$$

with N the number of data points. Thus, we define a time window of a width $2n + 1$ for which the rms value is calculated. The choice of the window width is not critical, but it should not be too small to smooth the signal noise sufficiently and should not be too large, otherwise the possible time dependence of m_i and m_{Mi} is lost. The scatter of these values obtained for different excitations lies within 5% and, therefore, this procedure is done several times before each test and the mean values are taken.

This method only allows the compensation for sting oscillations with frequencies less than the first resonance frequency of the system model balance. The transfer function between the measured acceleration and resulting force is constant for low frequencies (up to 400 Hz) but starts changing when it comes close to the first natural frequency together with a phase shift. The phase shift between the signals starts close to 0 deg and amounts to 180 deg for high frequencies. It is not possible to compensate all occurring inertia forces with the transfer function that was determined from the calibration tests because the recording time is too short during the real tests to have the same Fourier transformation. Thus, the transfer factors for the low frequencies (determined with the procedure described) are used for the complete spectrum. This leads to a compensation of the model support oscillations together with a possible amplification of frequencies close to and above the lowest resonance frequency of the system model balance. Thereupon, after the compensation a procedure is necessary to read a value for the aerodynamic coefficient that consists of the aerodynamic load and the inertia force part due to the model oscillations. A reliable method to achieve the steady part of the signal is the calculation of an adapted floating average over a time window that corresponds to the period of the lowest natural frequency visible in the signal. This yields a usable reduction

time that is equal to the test time window reduced by one half of the smoothing length on both sides.

For the assessment of this method it is necessary to compare the results obtained with other acceleration compensation methods. For this reason the results are compared with a method that uses accelerometers installed inside of the model (capsule model only).

B. Model-Based Acceleration Compensation

Here the model has to be equipped with six accelerometers to measure all components of the model acceleration. The idea of this method is to calculate the relations between the measured accelerations and the resulting forces directly from the specific test data [see Eq. (6)]. This method was developed by the Laboratoire de Recherches Balistique et Aérodynamique at Vernon, France. The 36 components of the matrix of inertia are found by a least-squares fit from the recorded data. Thus, there is no information necessary about the vibrating mass, the position of the center of gravity, or the moments of inertia for the vibrating system. The three basic assumptions are as follows.

1) The model behaves as a rigid body, i.e., the vibrations result only from the elasticity of the balance.

2) The model rotation rates p, q, and r around the coordinate axes can be neglected with respect to the angular accelerations p', q', and r'.

3) The aerodynamic coefficients are constant during the time window used for computing the least-squares fit.

With these assumptions the following equation can be written to describe the signals measured by the balance:

$$Z_i(t) = kc_i S_{\text{ref}} p_{t2}(t) + \sum_{j=1}^{6} A_{ij} a_j(t), \qquad i = 1, 2, \ldots, 6 \quad (6)$$

where Z_i is the measured balance loads, c_i the aerodynamic coefficients, S_{ref} the reference area, A_{ij} the elements of the inertia matrix, and a_j the measured accelerations. There are 42 unknowns and only 6 equations. This system is solved using the least squares method. The problem can be solved for the total test time window or for parts of it. In this case the time independence of the aerodynamic coefficients is not necessarily assumed for the total time window but only for parts of the time window considered. The influence of the window width on the results has to be checked. If the time window used for the least-squares fit of Eq. (6) is too small, low-frequency accelerations may not be recognized. This will be shown with the results of the capsule measurements in the shock tunnel TH2.

VI. Experimental Results

The overall accuracy of the force and moment coefficients presented is mainly restricted by the determination of the dynamic pressure[12] with an error of ±2.5% at condition I and ±5% at conditions IV and VII and the error in the calculation of the aerodynamic coefficients due to the dynamic response of the system-model–balance-model support. An estimate for this error was made by performing repeatability tests and is given subsequently for each model. Other error sources such as the uncertainty in model geometry, position of the balance in the model and angle of attack, A/D conversion (12 bit), balance calibration, and interference calculation amount to less than 1%.

The influence of the diverging flowfield produced by the conical nozzle on the forces and moments acting on the model is checked using the Newtonian flow theory. First, the aerodynamic loads are calculated for a parallel flow; thereafter, the loads are determined influenced by the flow angularity and the axial gradients, achieved by a nozzle flow calibration. To calculate aerodynamic coefficients for the conical nozzle case one has to choose an axial reference position, which for equal dynamic pressure of both parallel and conical nozzle flow at this position yields nearly the same aerodynamic coefficients. For the cone model and the capsule, this point could be chosen in a way that the difference between the two results is less than 1% for all angles of attack. For the ELAC I model the moment measured is additionally corrected with the ratio of the moments for the two flowfields determined after the location of the measuring point for the dynamic pressure is optimized for the forces. In this case the differences to correct are less than 2%.

A. Results of the Cone Measurements in TH2

The first experiments with the cone were performed at condition I (Table 1) with angles of attack ranging from 0 to 40 deg. At this stage, balance and model were not equipped with accelerometers. For these tests the pitot pressure and the stagnation point heat flux are measured with permanent probes 144 mm behind the cone tip to compensate for the diverging flowfield of the conical nozzle. Figure 5 shows a typical trace of the lift coefficient at 20-deg angle of attack. The oscillations of the model support system are clearly visible with a period of approximately 4 ms. The actual test time of this condition for performing pressure and heat flux measurements is about 5 ms. For force measurements a longer measuring time can be used as shown subsequently with the compensated measurements. The real value of the aerodynamic coefficients for these tests are determined by an adapted floating average calculation as described earlier (solid line in Fig. 5; the remaining data reduction time is indicated by the two vertical bars).

Jones[8] calculated lift and drag coefficients for a sharp cone with 30-deg cone angle assuming an inviscid flow with $\gamma = 1.4$, with an angle of attack between 0 and 15 deg at $M_\infty = 8$ (Fig. 6). The small deviation between the measured and calculated values may be due to viscous effects and the influence of the model sting. Figure 6 shows the measured drag and lift coefficients compared with the values of Jones[8] and two experimental data sets of Arrington et al.,[9] who performed measurements in helium at $M_\infty = 20$, $0 < \alpha < 16$ deg, and of Ladson and Blackstock,[10] who performed measurements in air at $M_\infty = 9.8$, $0 < \alpha < 40$ deg. As expected the measured drag coefficient is slightly higher than the calculated one, the offset is increasing with angle of attack. The experimental values of Arrington et al.[9] and Ladson and Blackstock[10] show a good agreement

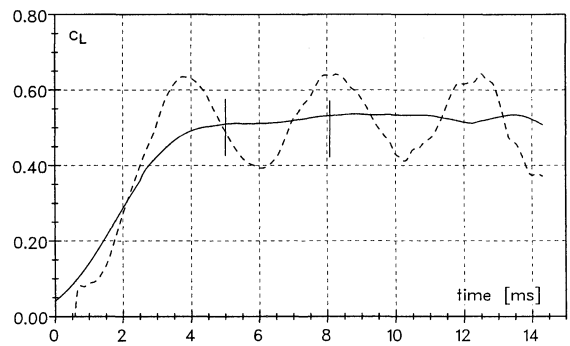

Fig. 5 Lift coefficient of the cone model at α = 20 deg, condition I: ——, floating averaged calculation and – – –, raw data.

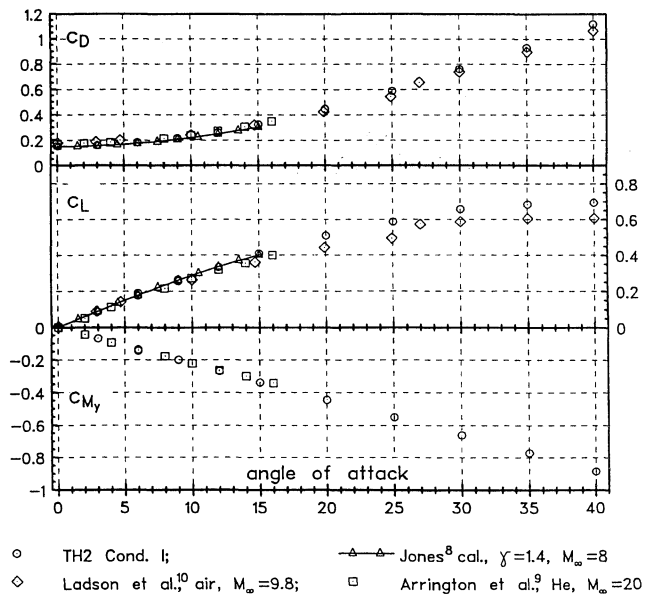

Fig. 6 Aerodynamic coefficients of the cone model for $\alpha = 0-40$ deg, condition I.

with the measurements of this paper. The lift coefficients measured in TH2 are equal to the calculated ones, whereas the compared experimental values are slightly smaller. Figure 6 also shows the pitching moment coefficient compared with values of Arrington et al.[9] The agreement achieved is as good as for the drag coefficient.

Further experiments were performed at 3-deg angle of attack for conditions I and IV (Table 1). The balance sting was equipped with two accelerometers which were used to perform a compensation for the low-frequency sting oscillations as described in Sec. V.A. In Fig. 7 an uncompensated lift coefficient history is shown together with the compensated one measured at condition I. The low-frequency oscillations are obviously well compensated, and the resulting coefficient shows a more or less steady behavior up to 13 ms. This justifies the use of the longer data reduction time for force measurements than for pressure and heat flux measurements. This elongation of the measuring time for force measurements is only possible at condition I, where the test gas drainage takes longer than 15 ms and no real gas effects appear. At condition IV there is only a period of 2 ms in which the high-stagnation temperature can be sustained and the test gas drainage time is about 4.5 ms. Hence, for this condition 2-ms actual measuring time is also valid for force measurements, and a data reduction without compensation for the sting oscillations would yield unreliable results. Figure 8 shows the time histories of the uncompensated and the compensated lift coefficient for this high-enthalpy test condition. It is obvious that the low-frequency oscillation is well compensated, and the resulting lift coefficient is steady throughout the measuring time. Figure 9 compares the sting gauge compensated coefficients of the six tests at conditions I and IV with the calculated results from Jones[8] (c_D, c_L) and with the data of Arrington et al.[9] (c_{M_y}). The repeatability of the results is within ±3% for the drag and ±5% for lift and pitching moment.

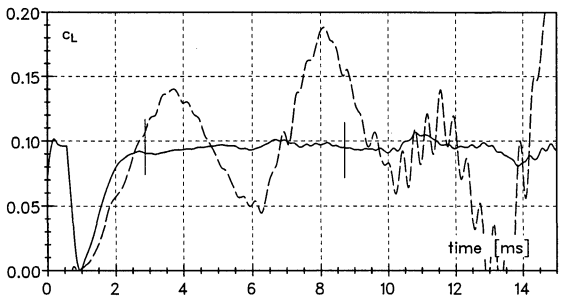

Fig. 7 Lift coefficient of the cone model at α = 3 deg, condition I: ——, sting gauge compensated data and – – –, uncompensated data.

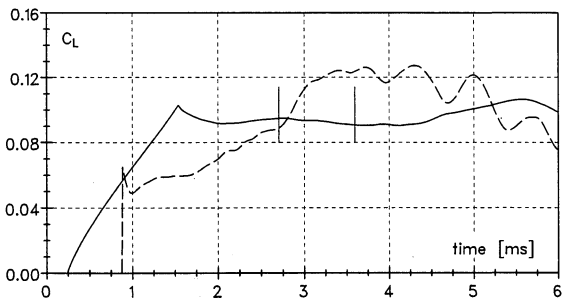

Fig. 8 Lift coefficient of the cone model at α = 3 deg, condition IV: ——, sting gauge compensated data and – – –, uncompensated data.

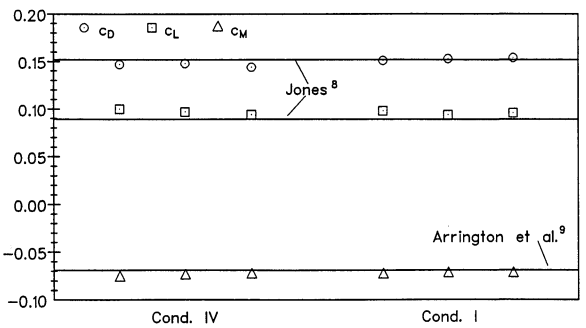

Fig. 9 Aerodynamic coefficients of the cone model at α = 3 deg; three repeatability tests at each condition I and condition IV.

B. Experiments with the Apollo Capsule Model

1. Measurements in Shock Tunnel TH2

The first set of experiments was performed at condition I and covered angles of attack ranging from 0 to 40 deg with three repeatability tests at α = 25 deg. The model was equipped with six accelerometers (see Fig. 3). The results obtained with the model compensation technique of Sec. V.B depend on the window period used for the least squares fit (Fig. 10). For this method the length of the time window to evaluate Eq. (6) has to be chosen wide enough to capture the low-frequency oscillations of the model support system. With a 4-ms window period the result is obviously wrong, whereas 7.5-ms reduction time leads to a result that does not change much when the reduction time is extended to 13 ms. The difference due to the different time windows is visible at the beginning of the plot. The difference is remarkable for the result obtained with the sting gauge compensation where the mean value is lower. This effect is caused by a low-frequency acceleration in Z direction starting at 1.5 ms together with the flow onset that is detected by the Z-direction gauge. The model-based compensation method leads to an incorrect interpretation of the signals because the low-frequency acceleration starting at 1.5 ms is not taken into account by the least squares procedure. The obtained curve fit is closer to the raw coefficient data because the low-frequency offset in the data is not detected. A summary of all condition I tests in TH2 is shown in Fig. 11 for c_a, c_n, and c_{M_y} as functions of the angle of attack together with experimental data for the Apollo command module (CM) of Moseley et al. (Ref. 11, Fig. 7). The axial coefficient shows a systematic

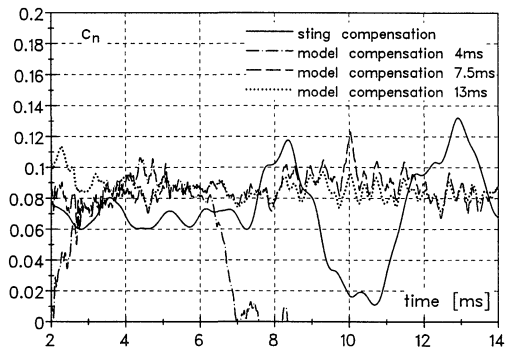

Fig. 10 Normal force coefficients of the capsule model obtained with the sting gauge compensation method compared to values calculated with the model gauge compensation method for three different time windows; α = 20 deg, condition I.

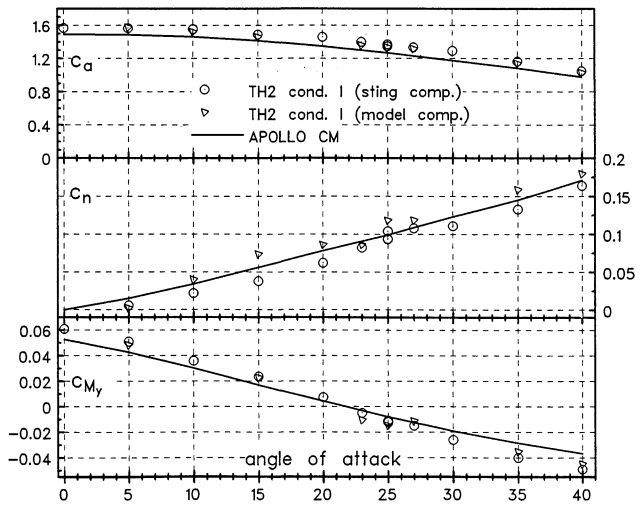

Fig. 11 Aerodynamic coefficients of the capsule model for $0 < \alpha < 40$ deg at condition I compared with Apollo CM data.

offset from the reference data. A possible reason for this is the balance sting that replaces the rear part of the capsule and increases the measured drag coefficient. The difference betweeen the results obtained with model compensation and sting compensation is small, just as for the pitching moment coefficient. For the normal force coefficient model compensation systematically gives a higher value. For 25-deg angle of attack several repeatability tests have been performed, c_a stays within a scatter of 6%, c_n varies about 20%, and c_{M_y} differs about 5%. To have reliable aerodynamic coefficients, it is advisable to have some repeatability tests.

2. Measurements in VKI Longshot

At the VKI, tests with the same capsule model have been performed at 20- and 25-deg angle of attack. The tunnel was operated at four different test conditions, two with nitrogen (LSCN 1 and LSCN 3) and two with carbon dioxide (LSCN 2 and LSCN 4) as test gas (see Table 2). The test conditions were designed for two different values of the viscous interaction parameter $\bar{V}^*$, however, using the same for one nitrogen and one carbon dioxide condition ($\bar{V}^* = 0.013$ for LSCN 1 and LSCN 2 and $\bar{V}^* = 0.02$ for LSCN 3 and LSCN 4) to investigate the influence of varying γ. For each condition and angle of attack two tests were performed to check the repeatability of the results. The recorded data were processed with both methods to compensate for the inertia forces resulting from the model support oscillations. Figure 12 shows the results for 25-deg angle of attack of all tests made in VKI Longshot and TH2 in comparison with the corresponding Apollo data.[11] For some VKI tests the resulting values are given for both procedures. They are equivalent for c_a whereas there is a systematic difference visible in c_n. All values achieved with the sting compensation method are smaller than those obtained with the model compensation method. This may also be due to low-frequency oscillations, which are not detected by the model compensation method. The results show the same behavior at 20-deg angle of attack. The effects of γ and $\bar{V}^*$ are different for c_a, c_n, and c_{M_y}. For c_a and c_n the values increase with increasing $\bar{V}^*$ and decreasing γ, whereas for c_{M_y} the results decrease with increasing $\bar{V}^*$ without a clear influence of γ. These effects do not exist in the TH2 measurements even though $\bar{V}^*$ at condition VII is three times higher than at conditions I and IV.

C. Force Measurements with the ELAC I Model

With the ELAC I model a first attempt was made to measure aerodynamic forces of this configuration with relatively low natural frequencies in shock tunnel TH2. Because of the lowest natural frequency of 140 Hz, compensation for the model support oscillations with gauges on the balance sting is not possible. Inertia forces resulting from the balance elasticity may not be separated

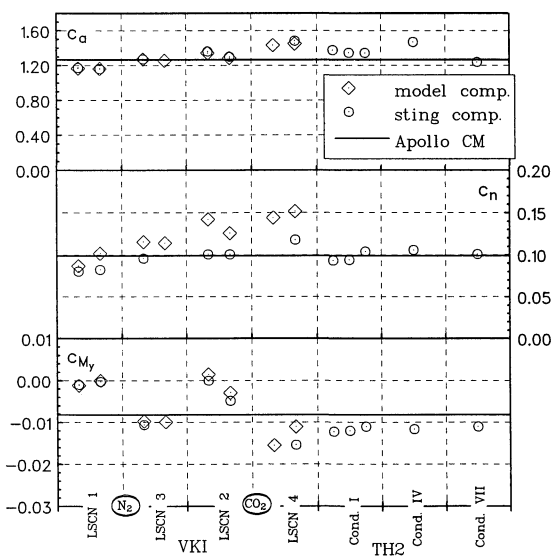

Fig. 12 Aerodynamic coefficients of the capsule model for α = 25 deg, VKI Longshot and TH2 tests.

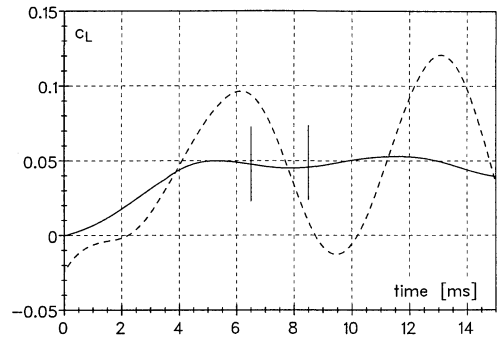

Fig. 13 Lift coefficient of the ELAC I at α = 6 deg, condition I: ——, floating averaged calculation and – – –, raw data.

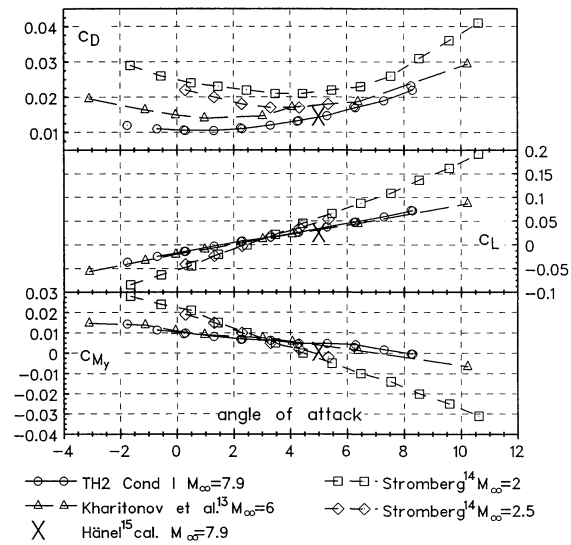

Fig. 14 Aerodynamic coefficients of the ELAC I model.

from the model support system oscillations that are measured by accelerometers on the balance sting. The signals of the balance will not correlate with the accelerations measured on the sting. Hence, in this case a long measuring time is necessary to determine the steady aerodynamic coefficients with the calculation of an adapted floating average over a time window of 7 ms length (corresponding to 140 Hz). As a typical example, Fig. 13 shows the time histories of both the averaged and raw lift coefficient. For all tests the value of the coefficients was taken at 7 ms. The results are compared with experimental data of Kharitonov et al.[13] and Stromberg,[14] obtained in different blow-down wind tunnels (Fig. 14). A Navier–Stokes calculation is only available[15] for α = 5 deg, $M_\infty = 7.9$, and $Re_{L_m} = 1 \times 10^6$. Kharitonov et al.[13] performed tests at $M_\infty = 6$ and $Re_{L_m} = 3 \times 10^6$, whereas Stromberg[14] measured at $M_\infty = 2$, $M_\infty = 2.5$, and $Re_{L_m} = 3 \times 10^6$. The measured drag coefficient decreases with increasing Mach number (Fig. 14), and the calculated value of Hänel et al.[15] is in good agreement with the results of this paper. The lower drag coefficient in the TH2 measurements may also be a result of the lower Reynolds number, which leads to a fully laminar flow. If the flow is partially turbulent, as in the tests of Stromberg[14] and Kharitonov et al.,[13] the local skin-friction coefficient c_f would be significantly higher leading to a higher drag coefficient. The derivative $dc_L/d\alpha$ decreases with increasing Mach number. For $M_\infty = 2$ it is 1.29, and for $M_\infty = 7.9$ it is 0.62. This is consistent with the theoretical values of $dc_L/d\alpha$ for a flat delta wing that may be calculated to[16]

$$\frac{dc_L}{d\alpha} = \frac{2\pi \tan\epsilon}{\int_0^{\pi/2} \sqrt{1 - \left[1 - \left(\tan\epsilon \sqrt{M_\infty^2 - 1}\right)\right]^2 \sin^2\varphi}\, d\varphi} \tag{7}$$

which yields a value of 1.41 for $M_\infty = 2$ and 0.67 for $M_\infty = 7.9$.

VII. Concluding Remarks

The measurements on a cone model at condition I in the shock tunnel TH2 showed that it is possible to determine aerodynamic loads without compensation for inertia forces caused by the oscillations of the model support system provided that the measuring time is longer than the period of the lowest natural frequency of the system-model balance. Measurements at high-enthalpy conditions with 1–2 ms test time require compensation for these inertia forces. The method presented in Sec. V.A using acceleration gauges on the balance sting successfully compensates these inertia forces and gives reliable results of good repeatability, as shown by the cone and capsule measurements at conditions I and IV. The results obtained are in good agreement with the presented reference data. This method does not require an extensive instrumentation of the force models used and, therefore, may be optimized in terms of weight and moment of inertia leading to a higher natural frequency and, thus, to a more reliable measurement. The comparison with a compensation method that is based on measured accelerations of the model (Sec. V.B) gives no significant improvement of the results. For the ELAC I tests the balance was used as an external sting mounted one. No compensation was possible for the occurring inertia forces due to the low resonance frequency of the model external balance system. The results obtained with the floating average calculation are in good agreement with the presented reference data.

Acknowledgments

Part of this work was supported by the Deutsche Forschungsgemeinschaft DFG within the Collaborative Research Center 253 Fundamentals of the Design of Aerospace Planes as well as by European Space Agency/European Space Technology Center within the Manned Space Transportation Program, Contract 11080/94/F/WE. We are also very grateful to J. M. Charbonnier, von Kármán Institute Brussels, for many helpful discussions and to S. Paris for performing the experiments in the VKI Longshot facility.

References

[1]Naumann, K. W., Ende, H., Mathieu, G., and George, A., "Further Developments of the ISL Millisecond Aerodynamic Force Measurement Technique," *Shock Waves at Marseille*, edited by R. Brun and L. Z. Dumitrescu, Springer, Berlin, 1995, pp. 281–286.

[2]Mee, D. J., Daniel, W. J. T., and Simmons, J. M., "Three-Component Force Balance for Flows of Millisecond Duration," *AIAA Journal*, Vol. 34, No. 3, 1996, pp. 590–595.

[3]Jessen, C., and Grönig, H., "A Six Component Balance for Short Duration Hypersonic Facilities," *New Trends in Instrumentation for Hypersonic Research*, edited by A. Boutier, Kluwer, Dordrecht, The Netherlands, 1993, pp. 295–305.

[4]Olivier, H., and Grönig, H., "Description of the Aachen Shock Tunnel TH2," Shock Wave Lab., Rheinisch–Westfälische Technische Hochschule, Aachen, Germany, Feb. 1995.

[5]Simeonides, G., "The VKI Hypersonic Wind Tunnels and Associated Measurement Techniques," von Kármán Inst., TM 46, Brussels, Nov. 1990.

[6]Charbonnier, J. M., and Paris, S., "The Longshot Tunnel Operated with Variable γ Testing Gases. Definition of Standard Operating Conditions," Progress Rept. HT-TN-E34-221-VKIN, MSTP II, European Space Agency, Rhode Saint Genese, Belgium, March 1996.

[7]Schnabl, F., "Entwicklung eines Algorithmus zur Auswertung der Eichversuche an 6–Komponenten–DMS–Waagen," *Journal of Flight Sciences and Space Research*, Vol. 11, No. 5, 1987, pp. 342–346.

[8]Jones, D. J., "Tables of Inviscid Supersonic Flow About Circular Cones at Incidence, $\gamma = 1.4$," AGARDograph 137, Pt. I, AGARD, London, 1969.

[9]Arrington, J. P., Joiner, R. C., Jr., and Henderson, A., Jr., "Longitudinal Characteristics of Several Configurations at Hypersonic Mach Numbers in Conical and Contoured Nozzles," NASA TN D-2489, Sept. 1964.

[10]Ladson, C. L., and Blackstock, T. A., "Air-Helium Simulation of the Aerodynamic Force Coefficients of Cones at Hypersonic Speeds," NASA TN D-1473, Oct. 1962.

[11]Moseley, W. C., Jr., Moore, R. H., Jr., and Hughes, J. E., "Stability Characteristics of the Apollo Command Module," NASA TN D-3890, March 1967.

[12]Olivier, H., "An Improved Method to Determine Free Stream Conditions in Hypersonic Facilities," *Shock Waves*, Vol. 3, No. 2, 1993, pp. 129–139.

[13]Kharitonov, A., Brodetsky, M., Krause, E., and Jacobs, M., "An Experimental Investigation of ELAC I Model at Supersonic Speeds," Rheinisch–Westfälische Technische Hochschule, TR A-96-10, SFB 253, Aachen, Germany, 1996.

[14]Stromberg, A., "Experimentelle Untersuchungen an der Hyperschallkonfiguration ELAC I bei Unter- und Überschallanströmung," Dr.-Ing. Dissertation, Aerodynamisches Institut, Rheinisch–Westfälische Technische Hochschule, Aachen, Germany, 1994.

[15]Hänel, D., Henze, A., and Krause, E., "Supersonic and Hypersonic Flow Computations for the Research Configuration ELAC I and Comparison to Experimental Data," *Journal of Flight Sciences and Space Research*, Vol. 17, No. 2, 1993, pp. 90–98.

[16]Schlichting, H., and Truckenbrodt, E., *Aerodynamik des Flugzeuges, Band II*, Springer–Verlag, Berlin, 1960, pp. 190, 191.

G. Laufer
Associate Editor